ChemComm

COMMUNICATION

Extremely efficient crystallization of HKUST-1 and Keggin-loaded related phases through the epoxide route†

Víctor Oestreicher[a] and Matías Jobbágy*[ab]

Cite this: *Chem. Commun.*, 2017, 53, 3466

Received 26th January 2017,
Accepted 27th February 2017

DOI: 10.1039/c7cc00737j

rsc.li/chemcomm

Highly crystalline HKUST-1 and COK-16-like phases were obtained based on a mild *in situ* alkalinization one-pot epoxide driven method. A slurry composed of finely ground trimesic acid, H_3BTC, dispersed in a $CuCl_2$ aqueous solution quantitatively developed well crystallized HKUST-1 after the addition of propylene oxide. The use of solid H_3BTC ensures a low concentration of free linker, favoring crystalline growth over the precipitation of amorphous or metastable impurities. An extreme space-time yield of 2.1×10^5 kg m^{-3} day^{-1} was reached, with no linker excess and minimum use of solvent. The method was equally efficient in the achievement of pure NENU/COK-16 phases, containing $[PW_{12}O_{40}]^{3-}$, $[PMo_{12}O_{40}]^{3-}$ and $[SiMo_{12}O_{40}]^{4-}$ polyoxometalates.

For several decades, research in advanced materials chemistry has been used to develop well-defined, systematically explored and reliable synthetic procedures. In recent days, the exploration of efficient and ecofriendly procedures has gained attention;[1] successful strategies were implemented in the case of mesoporous silica[2] or TiO_2 particles.[3] However, certain relevant materials such as Metal Organic Frameworks (MOF) have shown limited progress.[4] Among them, a highly valuable member of the MOF family, HKUST-1 or $Cu_3(BTC)_2(H_2O)_3$[5,6] is currently being produced at the industrial level through the electrolytic oxidation of metallic copper in the presence of H_3BTC alcoholic solution.[7] Recently, an alternative process, based on the spontaneous heterogeneous acid–base reaction of a slurry containing an excess of H_3BTC solution and $Cu(OH)_2$ microparticles, was used to develop this MOF phase reaching a space-time yield (STY) that dramatically improves the industrial procedure.[8] The process is equally successful in the preparation of $Fe(BTC)(H_2O)_3$ MOF.[9] In an effort to develop a greener synthesis avoiding commonly employed solvents such as DMF, strictly aqueous-based procedures were proposed. A suspension of H_3BTC in water reacted with different soluble Cu(II) salts to form HKUST-1, reaching a space-time yield (STY) of 1.7×10^3 kg m^{-3} day^{-1}.[10] In recent days, mechanochemical approaches based on the stoichiometric reaction of $Cu(OH)_2$ and H_3BTC reached exceptional STY values, minimizing the use of an organic solvent.[11] Notwithstanding, the texture of the products was far from being acceptable.

Inspired by the successful concepts implemented in the aforementioned reports, we conceived and evaluated a novel synthesis that leads to pure and highly crystalline $Cu_3(BTC)_2(H_2O)_3$ (CuBTC in the following) phases with extremely enhanced STY. The process is based on mild *in situ* alkalinization, driven by chloride-assisted epoxide ring rupture, without external heating (see Scheme 1).[12] The method was also applied to the preparation of the Keggin-polyoxometalate loaded forms of this MOF,[13] known as NENU[14] (or COK-16[15] phases). These functional structures are intrinsically valuable since they exhibit enhanced stability towards thermal decomposition[15] while the entrapped Keggin structure brings molecular catalysis activity under size-selective conditions provided by the MOF host.[14]

The method consists in the starting slurry composed of finely ground solid H_3BTC being dispersed in aqueous solutions containing $CuCl_2$. Keeping in mind the minimization of aromatic waste effluents, a stoichiometric $CuCl_2$ to H_3BTC ratio was employed in each batch throughout this study, exclusively. Secondly, the addition of propylene oxide (PO) drives the precipitation of

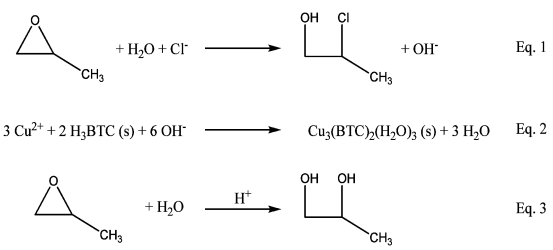

Scheme 1 Chloride attack and PO ring rupture driven alkalinization (1), H_3BTC deprotonation and HKUST-1 precipitation (2) and parallel acid catalyzed PO hydrolysis (3).

[a] *INQUIMAE-DQIAQF, Facultad de Ciencias Exactas y Naturales, Universidad de Buenos Aires. Ciudad Universitaria, Pab. II, C1428EHA, Buenos Aires, Argentina. E-mail: jobbag@qi.fcen.uba.ar*

[b] *Centro Interdisciplinario de Nanociencia y Nanotecnología, Argentina*

† Electronic supplementary information (ESI) available. See DOI: 10.1039/c7cc00737j

CuBTC according to the set of reactions depicted in Scheme 1. If the starting slurry also contains the soluble acid forms of Keggin anions, an analogous precipitation sequence can be defined for COK-16 phase formation (see the ESI,† Scheme S1).

In aqueous media, the rate of the first reaction is proportional to chloride and epoxide concentrations, rising pH above values of 11 (Scheme 1, eqn (1)).[16] In the present case, the second (coupled) reaction is limited by the rate of deprotonation/dissolution of the solid H_3BTC reagent and the subsequent precipitation of CuBTC (Scheme 1, eqn (2)). Since the undesired diol formation (Scheme 1, eqn (3)) competes with precipitation, an excess of epoxide is typically employed to ensure a high precipitation yield.[12,16] In a typical procedure, 10 g of $CuCl_2{\cdot}2H_2O$ were dissolved in 16.9 mL of H_2O; 8.2 g mesh ground solid H_3BTC were added to the former solution under vigorous stirring. 12.3 mL of PO were added to the stirred slurry and left to react for 5 minutes. The blue solid produced was washed and centrifuged three times with 15 mL of water. The other experimental conditions evaluated (see the ESI,† Table S1) resulted in lower precipitation yields and/or undesired impurities. The described procedure was extended to prepare the COK-16 phase by adding a stoichiometric content of soluble $H_3PW_{12}O_{40}$ in the starting $CuCl_2/H_3BTC$ slurry (see the ESI,† Table S1); the product collected and washed will be referred to as the sample PW-CuBTC along the text. The precipitation process is faster in this case, despite the higher initial acidity; the ability of Keggin anions, $[AM_{12}O_{40}]^{m-}$, to induce and drive the nucleation and growth, even under conditions in which the HKUST-1 cannot be obtained is well documented.[17] In every case, control experiments in the absence of PO resulted in neither precipitation nor H_3BTC dissolution. Fig. 1 depicts FESEM images of the obtained solid; both samples revealed well-defined truncated octahedral micrometric crystals, exclusively.

The procedure was equally efficient for the preparation of $[PMo_{12}O_{40}]^{3-}$ and $[SiMo_{12}O_{40}]^{4-}$ loaded forms (see the ESI,† Fig. S1). The crystals inspected by EDS probe revealed a Cu : W : P ratio in excellent agreement with expected values of a pure $[Cu_3(BTC)_2]_4(PW_{12}O_{40})Cu_{3/2}$ (COK-16) phase (see the ESI,† Fig. S2); similar results were observed for the Cu : Mo : P ratio of the sample MoP-CuBTC (see the ESI,† Fig. S3). ICP analysis confirmed the elemental ratio of all samples. PXRD images of samples CuBTC and PW-CuBTC are presented in Fig. 2, revealing the precipitation of Cu(II) in the form of highly crystalline HKUST-1 and COK-16, respectively. No traces of remnant H_3BTC nor related Cu(II)-based side products, as $Cu_2Cl(OH)_3$, $Cu(HBTC)(H_2O)_3$ or $Cu_2(BTC)(OH)(H_2O)$ were observed (see the ESI,† Fig. S4).

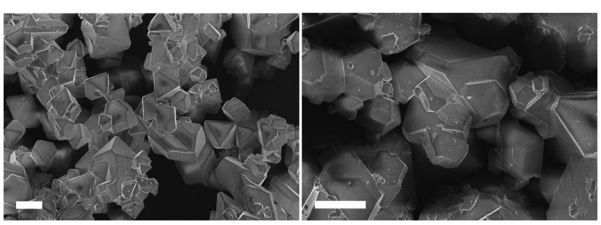

Fig. 1 FESEM images of the samples CuBTC (left) and PW-CuBTC (right). Scale bar represents 5 μm for both images.

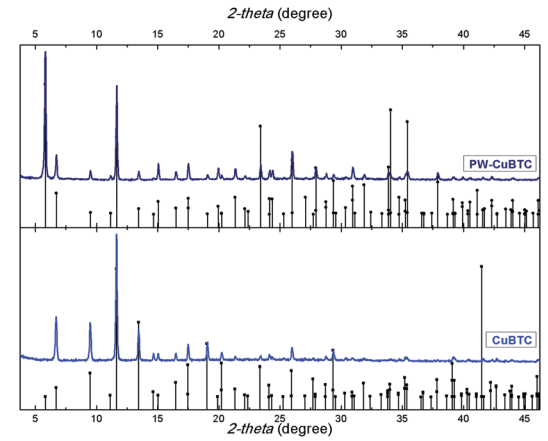

Fig. 2 PXRD images of samples for the samples CuBTC (lower pattern) and PW-CuBTC (upper pattern). Reference diffraction lines from HKUST-1 and COK-16 reference phases are also presented.

In order to further analyze the obtained phases, thermogravimetric analysis (TGA) was performed for both samples. For each sample, two main mass loss steps were observed (see the ESI,† Fig. S5). The first mass loss (31% for CuBTC and 21% for PW-CuBTC) recorded below 200 °C involved reversible departure of water molecules, either coordinated to Cu(II) ions or hosted within the micropores. The second mass loss step (64% for CuBTC and 30% for PW-CuBTC), resulted from the irreversible decomposition of BTC linkers, in excellent agreement with values reported elsewhere.[14,15] No net mass loss corresponding to remnant H_3BTC was observed, in agreement with PXRD inspection, confirming the purity of the samples (see the ESI,† Fig. S6). Fig. 3 presents nitrogen sorption isotherms of both samples. Microporous structures (according to a well-defined Type I isotherm) with large surface areas of 2100 and 1150 $m^2\ g^{-1}$, for CuBTC and PW-CuBTC samples respectively were observed.[7] The lower value of the former obeys the quantitative load of $[PW_{12}O_{40}]^{3-}$ Keggin into type A pores of the CuBTC host lattice.[14] Reference COK-16 and NENU-3 phases prepared following the original reported procedures presented similar sorption isotherms (data not shown).

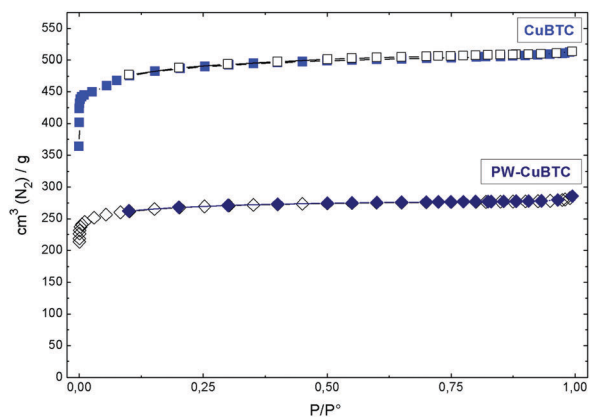

Fig. 3 N_2 adsorption (filled symbols)/desorption (empty symbols) isotherms recorded at 77 K for CuBTC and PW-CuBTC samples.

Table 1 Relevant methods and their inherent merits

Ref.	Cu(II) source	STY (kg m^{-3} d^{-1})	Enviromental factor	SI (kg_{Sv} kg_{MOF}^{-1})	WI
8	$Cu(OH)_2$	1842	28	18	8.9
10	$Cu(CH_3COO)_2{\cdot}H_2O$	2035	1192		1190
11	$Cu(OH)_2$	144 000	0.7	0.5	
CuBTC[a]	$CuCl_2{\cdot}2H_2O$	210 000	3.0		1.6
PW-CuBTC[a]	$CuCl_2{\cdot}2H_2O$	2570 000	1.2		0.7

[a] This work.

The whole precipitation process of CuBTC takes place in less than 5 min, resulting in a high STY value for HKUST-1 of 2.1×10^5 kg m^{-3} day^{-1}. The present method improves by one order of magnitude recent achievements,[8,10] and by three orders industrially employed procedures.[4] Sample PW-CuBTC developed precipitation in less than 1 min, despite the high initial acidity, reaching a STY of 2.6×10^6 kg m^{-3} day^{-1}.

Concerning the crystallization mechanism, the screening of pH along the precipitation of CuBTC revealed that a nucleation burst and subsequent growth takes place under acidic conditions, defined by a precipitation *plateau* fixed around pH 3.5 to 4.0, depending on the water activity (see the ESI,† Fig. S7). Regarding this, the formation of the present highly crystalline MOF phases can be understood to be the result of controlled dissolution of H_3BTC, mainly in the form of partially protonated linker moieties (see the ESI,† Fig. S8), ensuring a low supersaturation with respect to the MOF phase along the whole growth process. Moreover, the absence of undesired Cu(II) basic chlorides obeys the smooth rise of pH, preventing the excessive alkalinization under which the precipitation of this phase can take place.[18] This condition was systematically observed under diverse synthesis conditions, including different mixtures of EtOH–H_2O or less reactive epoxides as glycidol (see the ESI,† Fig. S9).[19]

Beyond the chemical aspects of the reaction, it is known that epoxide driven precipitation releases heat, increasing the temperature significantly.[19] In the present case, final temperatures of *ca.* 60 °C were reached within the first 3 min of reaction. Since the activation energy of chloride driven PO ring's rupture is *ca.* 70 kJ mol^{-1} (see the ESI,† Fig. S10), the autogenous heating recorded herein can accelerate the alkalinization rate by one order of magnitude. The rise of temperature also contributes to the enhancement of the dissolution rate of the solid H_3BTC reagent as well as the recrystallization of the formed phases.

Table 1 compares key parameters of the present method with those offering the highest STY values reported to date. Beyond the inherent yield, the environmental impact was assessed on the basis of well accepted key parameters[20,21] such as environmental factor (EF), and solvent (SI) or water intensity (WI), according to the current trends in materials chemistry.[3] An extended analysis employing other relevant indicative factors is available (see the ESI,† Table S2). From a comparative analysis, we can conclude that only the mechanochemical route's overall performance competes with the present one. However, the high quality and diversity of the phases obtained herein elevates the present method over previous standards.

Beyond the aspects discussed, the present method is well positioned in terms of the inherent costs, since the Cu(II) source is more cheaply available and the required PO represents less than 5% of the overall reagent's cost (see the ESI,† Table S3).

Additionally, the absence of non-volatile salts or H_3BTC excess after reaction offers the possibility of purification procedures based on low-pressure/mild temperature removal of chlorohydrin and 1,2 propanediol side products (see eqn (1) and (3)). The former can be recycled into PO by means of well established procedures belonging to the industrial production of epoxides.[22]

Summarizing, the epoxide route introduced herein allows the one-pot quantitative aqueous based preparation of highly crystalline HKUST-1 or COK-16 MOF phases achieving extreme space-time yields, with no aromatic waste effluents and minimum use of solvents.

This work was supported by the University of Buenos Aires (UBACyT 20020130100610BA), the Agencia Nacional de Promoción Científica y Tecnológica (ANPCyT PICT 2012-1167) and the National Research Council of Argentina (CONICET PIP 11220110101020). VO acknowledges CONICET for a doctoral fellowship. VO is member of ALN. MJ is a Research Scientist of CONICET (Argentina). We deeply acknowledge BASF company for generously supplying Basolite C300.

References

1 N. Baccile, F. Babonneau, B. Thomas and T. Coradin, *J. Mater. Chem.*, 2009, **19**, 8537–8559.
2 J. Jammaer, T. S. van Erp, A. Aerts, C. E. A. Kirschhock and J. A. Martens, *J. Am. Chem. Soc.*, 2011, **133**, 13737–13745.
3 M. Pini, R. Rosa, P. Neri, F. Bondioli and A. M. Ferrari, *Green Chem.*, 2015, **17**, 518–531.
4 A. U. Czaja, N. Trukhan and U. Müller, *Chem. Soc. Rev.*, 2009, **38**, 1284–1293.
5 S. S. Y. Chui, S. M. F. Lo, J. P. H. Charmant, A. G. Orpen and I. D. Williams, *Science*, 1999, **283**, 1148–1150.
6 L. Alaerts, E. Seguin, H. Poelman, F. Thibault-Starzyk, P. A. Jacobs and D. E. De Vos, *Chem. – Eur. J.*, 2006, **12**, 7353–7363.
7 U. Müller, M. Hesse, H. Puetter, M. Schubert, H. Wessel, J. Hu and G. Marcus, *US Pat.*, US 7968739 B2, 2011.
8 G. Majano and J. Pérez-Ramírez, *Adv. Mater.*, 2013, **25**, 1052–1057.
9 G. Majano, O. Ingold, M. Yulikov, G. Jeschke and J. Perez-Ramirez, *CrystEngComm*, 2013, **15**, 9885–9892.
10 J. Huo, M. Brightwell, S. El Hankari, A. Garai and D. Bradshaw, *J. Mater. Chem. A*, 2013, **1**, 15220–15223.
11 D. Crawford, J. Casaban, R. Haydon, N. Giri, T. McNally and S. L. James, *Chem. Sci.*, 2015, **6**, 1645–1649.
12 A. E. Gash, T. M. Tillotson, J. H. Satcher, J. F. Poco, L. W. Hrubesh and R. L. Simpson, *Chem. Mater.*, 2001, **13**, 999–1007.
13 L. Yang, H. Naruke and T. Yamase, *Inorg. Chem. Commun.*, 2003, **6**, 1020–1024.
14 C. Y. Sun, S. X. Liu, D. D. Liang, K. Z. Shao, Y. H. Ren and Z. M. Su, *J. Am. Chem. Soc.*, 2009, **131**, 1883–1888.
15 D. Mustafa, E. Breynaert, S. R. Bajpe, J. A. Martens and C. E. A. Kirschhock, *Chem. Commun.*, 2011, **47**, 8037–8039.
16 V. Oestreicher and M. Jobbágy, *Langmuir*, 2013, **29**, 12104–12109.
17 S. R. Bajpe, C. E. A. Kirschhock, A. Aerts, E. Breynaert, G. Absillis, T. N. Parac-Vogt, L. Giebeler and J. A. Martens, *Chem. – Eur. J.*, 2010, **16**, 3926–3932.
18 V. Oestreicher, I. Fábregas and M. Jobbágy, *J. Phys. Chem. C*, 2014, **118**, 30274–30281.
19 V. Oestreicher, M. Perullini and M. Jobbágy, *Dalton Trans.*, 2016, **45**, 9920–9924.
20 C. Jiménez-González, D. J. C. Constable and C. S. Ponder, *Chem. Soc. Rev.*, 2012, **41**, 1485–1498.
21 R. A. Sheldon, *Green Chem.*, 2017, **19**, 18–43.
22 D. Kahlich, U. Wiechern and J. Lindner, *Ullmann's Encyclopedia of Industrial Chemistry*, 2011.

